NUMERICAL ANALYSIS OF ATMOSPHERIC AEROSOL MONITORING USING HORIZONTAL SCANNING LIDAR

JOSEPH OOI BOON HAN

UNIVERSITI SAINS MALAYSIA

2025

NUMERICAL ANALYSIS OF ATMOSPHERIC AEROSOL MONITORING USING HORIZONTAL SCANNING LIDAR

by

JOSEPH OOI BOON HAN

Thesis submitted in fulfilment of the requirements
for the degree of
Doctor of Philosophy

February 2025

ACKNOWLEDGEMENT

I came into the programme as a fast-track candidate fresh out of the University of Cambridge, and I found out quickly that this PhD was an entirely different ball game. Without my supervisors, Dr Edmund Loh Wai Ming, Associate Professor Dr Wong Chow Jeng and Dr Ismail Ahmad Abir, this would have been a nightmare. Thank you for your help in getting acquainted with this subject, your pointers in navigating my research, your input when I had to change my PhD topic and your aid in navigating the administrative matters that cropped up towards the end of my studies.

I would also like to thank the School of Physics, Universiti Sains Malaysia, for providing me with the facilities and resources needed for this work. This research was funded by the Ministry of Higher Education, Malaysia, under the Fundamental Research Grant Scheme [Grant number FRGS/1/2019/STG02/USM/02/11]. A shout out to my colleagues in Engineering Lab 339 who have never failed to make my days there interesting, either by giving me computer components to reassemble or by taking me out for meals. I am also grateful to Dr Lim Lian Tze, whose LaTeX template I have used and modified with permission to compile my PhD thesis.

My heartfelt gratitude goes out to my parents and brother, who have supported me throughout this PhD journey with prayer and love. They stood beside me through the storms and encouraged me time and again to fix my eyes on God. They never ceased to pray for me and comfort me with Scripture when the going gets rough. They taught me to give thanks to God for bringing me thus far, and for them I give thanks as well. I also appreciate the prayer support of my church family in Penang. God bless you all.

Above all, all praise to God for sustaining and guiding me to this day when my labour has bore fruit. He is faithful. He is good. He is my strength. *Soli Deo Gloria*!

And whatever you do, in word or deed, do everything in the name of the Lord Jesus, giving thanks to God the Father through him. (Col. 3:17)

TABLE OF CONTENTS

LIST OF TABLES

Page

LIST OF FIGURES

LIST OF SYMBOLS

A	Area of receiver
D	LIDAR detection range
d_0	Dry scatterer diameter
d_{eff}	Effective scatterer diameter
E_0	Laser pulse energy
$f(\text{RH})$	Hygroscopic growth factor
$G_{\text{MS}}(r)$	Range-resolved ratio of multiple scattering LIDAR returns
$\overline{G_{\text{MS}}}$	Range-averaged ratio of multiple scattering LIDAR returns
$L_{\text{e},\Omega,\lambda}$	Solar spectral radiance
P_0	Initial laser power
P_B	Solar background noise
P_D	Detector noise
$P_{\text{SS}}(r)$	Range-resolved single scattering LIDAR signal power
$P_{\text{MS}}(r)$	Range-resolved multiple scattering LIDAR signal power
$q(r)$	LIDAR overlap function
r	LIDAR detection range
r_0	Full overlap distance
S	LIDAR ratio
V	Meteorological visibility
$\alpha(r)$	Total extinction coefficient
$\beta_\pi(r)$	Total backscattering coefficient
γ_{PM}	Weighted contribution of PM to multiple scattering

ϵ	Single-fit parameter for hygroscopic growth factor
η_{MS}	Multiple scattering correction factor
λ_{laser}	Laser wavelength
τ	Laser pulse width
ϕ	Mie scattering size parameter

LIST OF ABBREVIATIONS

AOD	Aerosol Optical Depth
API	Air Pollution Index
AQM	Air Quality Monitoring
BLIA	Bayan Lepas International Airport
CAQM	Continuous Air Quality Monitoring
EARLINET	European Aerosol Research LIDAR Network
EBL	Elastic Backscatter LIDAR
FWHM	Full-Width Half-Maximum
LALINET	Latin American LIDAR Network
LED	Light Emitting Diode
LIDAR	LIght Detection And Ranging
MCAQM	Mobile Continuous Air Quality Monitoring
MODIS	Moderate Resolution Imaging Spectroradiometer
MPE	Maximum Permissible Exposure
MPLNET	Micro-Pulse LIDAR Network
PBL	Planetary Boundary Layer
PM	Particulate Matter
PMT	Photomultiplier Tube
PWM	Pulse Width Modulation
RCS	Range-Corrected Signal
RH	Relative Humidity
RFOV	Receiver Field-of-View

SNR	Signal-to-Noise Ratio
SEA	Southeast Asia
USM	Universiti Sains Malaysia
w.r.t.	With Respect To

LIST OF APPENDICES

ANALISIS NUMERIK UNTUK PEMANTAUAN AEROSOL ATMOSFERA MENGGUNAKAN LIDAR IMBASAN MENDATAR

ABSTRAK

Pencemaran udara seperti jerebu kerap berlaku di negara-negara yang terdedah kepada kandungan bahan pencemar udara yang tinggi. Di Malaysia, jerebu berlaku apabila banyak aerosol atmosfera, terutamanya zarah-zarah terampai (PM), terhasil daripada sumber-sumber pencemaran tempatan dan luaran. Aerosol atmosfera boleh dipantau dengan menggunakan stesen pemantauan kualiti udara atau LIDAR atmosfera. LIDAR didapati mempunyai resolusi dan kadar pengukuran yang mantap untuk memantau aerosol atmosfera dengan lebih efektif berbanding dengan stesen pemantauan kualiti udara. Namun, LIDAR imbasan mendatar belum pernah diimplementasikan dalan pemantauan aerosol kerana ia masih belum dipakai secara meluas. Tanpa model numerik, peluang perkembangan dalam penggunaan LIDAR imbasan mendatar untuk pengesanan dan pemantauan aerosol atmosfera berterusan akan terjejas. Kajian ini bertujuan untuk membentangkan analisis numerik pemantauan aerosol atmosfera menggunakan LIDAR imbasan mendatar. Ini dapat dicapai melalui penilaian model pengesanan jerebu yang menganalisis kesan PM pada bacaan LIDAR imbasan mendatar semasa berjerebu. Justeru, keberkesanan LIDAR imbasan mendatar dalam pemantauan aerosol atmosfera boleh disahkan tanpa memerlukan peralatan fizikal. Pertamanya, penilaian numerik melalui kaedah kajian perbandingan dijalankan untuk menilai prestasi LIDAR imbasan mendatar hipotetikal berdasarkan teori penyerakan tunggal. Seterusnya, LIDAR hipotetikal disimulasikan dalam cuaca yang berbeza untuk mengenal pasti kesesuaian teori penyerakan berganda semasa menganalisis bacaan LIDAR imbasan mendatar bagi tujuan pengesanan jerebu. Selepas model pengesanan jerebu telah dikenal pasti, teori penyerakan berganda akan ditambah baik untuk menilai kesan kelembapan relatif (RH) pada bacaan LIDAR imbasan mendatar semasa berjerebu. Teori penyerakan berganda ini bertujuan untuk menentukan pembetulan model pengesanan jerebu LIDAR bagi mengelaskan jenis jerebu cuaca kering dan lembap. Kajian kes telah dijalankan dengan LIDAR imbasan mendatar hipotetikel yang mempunyai dua

panjang gelombang dan beberapa bidang penglihatan penerima (RFOV). Maklumat darjah penglihatan dan RH digunakan untuk mensimulasikan bacaan LIDAR hipotetikal semasa berjerebu. Keputusan kajian kes menunjukkan LIDAR hipotetikal ini dapat mencapai prestasi setanding dengan LIDAR atmosfera sebenar kerana jarak pengesanan mendatar maksimum waktu malam adalah sejauh 1 km untuk kedua-dua saluran panjang gelombang. Dalam analisis, teori penyerakan berganda dipakai untuk menentukan model pengesanan jerebu dengan memuratakan nisbah bacaan LIDAR semasa berjerebu mengikut jarak. Model pengesanan jerebu numerik didapati mencukupi untuk aplikasi secara praktikal kerana ia mampu mengklasifikasikan jerebu hingga ke tahap sederhana dengan menggunakan mana-mana LIDAR imbasan mendatar. Akhir sekali, pembetulan model pengesanan jerebu untuk RFOV paling lebar diungkapkan sebagai fungsi kuadratik RH dengan mengaplikasikan regresi polinomial dan Kriteria Maklumat Akaike. Analisis numerik ini cukup jelas menunjukkan bahawa LIDAR imbasan mendatar boleh digunakan dalam pemantauan aerosol atmosfera tanpa memerlukan sebarang pemasangan LIDAR fizikal.

NUMERICAL ANALYSIS OF ATMOSPHERIC AEROSOL MONITORING USING HORIZONTAL SCANNING LIDAR

ABSTRACT

Air pollution episodes like haze are common in countries exposed to high levels of air pollutants. In Malaysia, haze occurs when high concentrations of atmospheric aerosols, especially particulate matter (PM), are produced from local and transboundary sources. Atmospheric aerosols can be monitored using air quality monitoring stations or atmospheric LIDARs. LIDARs can potentially provide better atmospheric aerosol monitoring than air quality monitoring stations due to superior spatio-temporal resolutions and faster detection. However, horizontal scanning LIDARs in particular have yet to be implemented as aerosol monitoring tools because they are recently introduced. Furthermore, numerical models to establish empirical methods for using horizontal scanning LIDARs in continuous atmospheric aerosol detection and monitoring are unavailable. This study aims to present numerical analysis of atmospheric aerosol detection using horizontal scanning LIDAR. By evaluating haze detection models that analyze effects of PM present in haze on horizontal scanning LIDAR readings, effectiveness of horizontal scanning LIDARs in atmospheric aerosol monitoring can be assessed without physical units. Numerical assessment via comparative study method is first conducted to evaluate the performance of a hypothetical horizontal scanning LIDAR using single scattering theory. Then, the hypothetical LIDAR is simulated in different weather conditions to investigate the feasibility of incorporating multiple scattering theory when analyzing horizontal scanning LIDAR readings to detect haze. After establishing the haze detection model, multiple scattering theory is improved to assess effects of relative humidity (RH) on horizontal scanning LIDAR readings during haze. Improved multiple scattering theory is used to identify any corrections to the LIDAR haze detection model when classifying dry and humid haze. A case study is performed using a hypothetical dual-wavelength, multiple-receiver field-of-view (RFOV) horizontal scanning LIDAR. Expected hypothetical LIDAR readings obtained during haze are simulated using meteorological visibility and RH. Results show that this hypo-

thetical LIDAR has comparable performance to actual atmospheric LIDARs, achieving maximum nighttime horizontal detection range of 1 km for both wavelength channels. In the analysis, the LIDAR haze detection model is established using range-averaged ratio of LIDAR returns by incorporating multiple scattering LIDAR theory. This model can classify haze up to moderate levels using any horizontal scanning LIDAR, which suffices for practical applications. Lastly, model corrections for the widest RFOV are expressed as quadratic functions of RH using polynomial regression and Akaike Information Criterion. This numerical analysis has demonstrated that horizontal scanning LIDARs can be used in atmospheric aerosol monitoring without physically assembling any LIDARs.

CHAPTER 1

INTRODUCTION

This chapter introduces the background and motivation for conducting a numerical analysis of atmospheric aerosol monitoring using horizontal scanning LIght Detection And Ranging (LIDAR). In Section 1.1, the background of the study is covered to provide context for the need to conduct this research. The material in this section draws on the author's previous work (Ooi et al., 2025). After the research gap is identified, the problem statement is presented in Section 1.2, while the aim and objectives of this study are outlined in Section 1.3. Section 1.4 highlights the significance of conducting the study. Next, the scope of the numerical analysis of atmospheric aerosol monitoring using horizontal scanning LIDAR is defined in Section 1.5. Lastly, this chapter is concluded with an overview of the structure of this thesis in Section 1.6.

1.1 Background of the Study

Ambient air pollution, a side effect of rapid industrialisation and modernisation, poses a great risk to the environment and human health. Air pollution events are often attributed to high concentrations of atmospheric aerosols present in the air. Colbeck and Lazaridis (2010) define aerosols as stable suspensions of solid and liquid particles in a gas which can be anywhere between 0.001 and 100 μm in size. Atmospheric aerosols, as air pollutants, can be categorised as primary (directly emitted into the atmosphere) and secondary pollutants (formed from chemical reactions and microphysical processes in the air) (European Environment Agency, 2022). Sources of these air pollutants can be natural, anthropogenic, or both, with common culprits being the agricultural, industrial, automotive and waste treatment sectors, in addition to forest fires and volcanic eruptions (European Environment Agency, 2022; World Health Organization, 2022). Some examples of major atmospheric aerosols include particulate matter (PM), sulfur dioxide, nitrogen dioxide, ozone and black carbon.

According to World Health Organization (2022), PM is often chosen as a proxy indicator for air pollution levels over other atmospheric aerosols because it has the greatest impact on the human population compared to other pollutants. PM can be characterised using its size, specifically the 50% efficiency cut-off diameter when samples are passed through a size-selective inlet (Colbeck & Lazaridis, 2010). Usually, PM is understood to refer to two main size categories: PM_{10} that can reach aerodynamic sizes of at most 10μm and $PM_{2.5}$ that has a maximum aerodynamic diameter of 2.5μm. Based on these two size categories, World Health Organization (2022) has set threshold values for PM mass concentrations, listed in Table 1.1, to evaluate the danger level of polluted air.

Table 1.1: Air quality guideline values for PM mass concentration as defined by World Health Organization (2022).

PM Category	**Annual Mean (μg m^{-3})**	**24-Hour Mean (μg m^{-3})**
$PM_{2.5}$	5	15
PM_{10}	15	45

Malaysia is a victim of poor air quality as a result of frequent exposure to high concentrations of atmospheric aerosols produced from local and transboundary sources. Even on a normal, haze-free day, close to one third of the total number of air quality monitoring (AQM) stations in Malaysia record only moderate air quality (Air Pollution Index (API) between 51 and 100), with the worst-suffering regions concentrated in Penang and Kedah, near the North of Peninsular Malaysia (Department of Environment, 2025). For example, during the long and severe haze episode that encompassed Southeast Asia (SEA) in 2015, the highest mass concentration of $PM_{2.5}$ recorded as a 24-hour average was 136 μg m^{-3}. This reading was at least five times higher than ambient values of 14.3–24.5 μg m^{-3} measured during periods with no reported haze episodes (Latif et al., 2018). Numerous studies have established that atmospheric aerosols, particularly PM, have negative effects on human health. For example, Z. Chen et al. (2019) analyzed annual data in Jinan, China that showed increased prevalence

of respiratory diseases and lung function impairment among students in schools with higher levels of air pollution. PM is also shown to be positively correlated to adverse health-related problems observed during air pollution episodes, and has significant effects on morbidity and mortality (Colbeck & Lazaridis, 2010). Specifically, PM_{10} has been shown to produce free radicals and exert oxidative stress on the lungs (D. M. Brown et al., 2007). On the other hand, $PM_{2.5}$ is expected to be more dangerous than PM_{10} as their smaller aerodynamical sizes enable them to remain suspended in air for longer periods of time compared to PM_{10} (Colbeck & Lazaridis, 2010). Furthermore, $PM_{2.5}$ may penetrate deeper into the human bloodstream and cause systemic effects (Pope III et al., 2009; World Health Organization, 2022). A size comparison between $PM_{2.5}$, PM_{10} and everyday objects is shown in Figure 1.1.

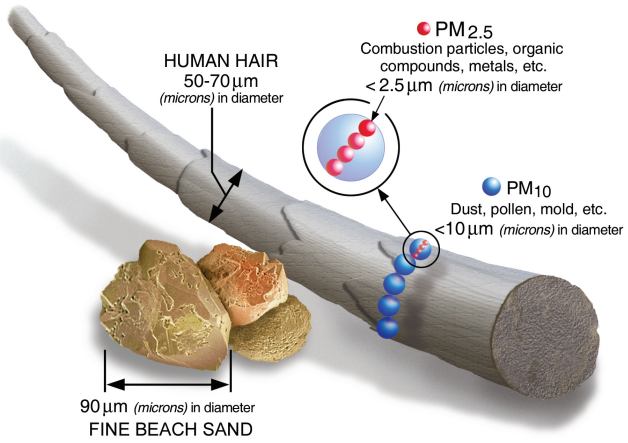

Figure 1.1: Size comparisons for $PM_{2.5}$ and PM_{10} with respect to human hair and a grain of sand. Used with permission from Environmental Protection Agency (2010).

PM poses indiscriminate health risks to people living in both urban and rural areas, as well as in both developed and developing countries alike. The dangers of PM and atmospheric aerosols in general have led to calls for better and faster atmospheric aerosol monitoring measures in order to protect public health. In Malaysia, 65 Continuous Air Quality Monitoring (CAQM) and three Mobile Continuous Air Quality Monitoring (MCAQM) stations are employed to provide continuous monitoring of air quality data (Pakar Scieno TW Sdn. Bhd., 2017). Atmospheric aerosol concentration measuring

instruments employed in AQM stations like CAQM and MCAQM stations conduct point measurements of pollutant concentrations using a variety of different measuring principles, such as gravimetric, optical, microbalance and electrical charge (Amaral et al., 2015). For instance, the particle analyser used by Pakar Scieno TW Sdn. Bhd. (2017) functions by first drying air samples that have been collected, filtering the samples according to size before using the microbalance technique to measure $PM_{2.5}$ and PM_{10} concentrations. These almost real-time measurements, often averaged over an hour, are then converted into API readings for further monitoring and public use (Academy of Sciences Malaysia, 2016). However, conventional AQM stations are only capable of conducting in-situ sampling and measurement of atmospheric aerosol concentrations. Consequently, results obtained from this point measurement technique are not representative of air quality further away from the station (Parracino et al., 2016).

In order to assess the climate impact and prevent adverse health effects that are introduced by atmospheric aerosols, information about their spatial distribution is often required to identify trends and improve forecast models (Colbeck & Lazaridis, 2010). To extend the effective detection range for atmospheric aerosol monitoring, one can use remote sensing techniques to detect aerosols like PM that are present in the air. For example, Wong et al. (2007) developed a passive remote sensing technique that used surveillance cameras to monitor air quality. While this method may have slightly longer detection ranges than conventional AQM stations, the accuracy of PM concentrations estimated from image data calibrations will largely depend on camera sensor and image processing quality. On the other hand, information like vertical distributions of atmospheric aerosols can be deduced to a certain extent from satellite data like aerosol optical depth (AOD). However, satellite monitoring techniques using equipment such as Moderate Resolution Imaging Spectroradiometer (MODIS) only have poor temporal resolutions down to one day (Land Processes Distributed Active Archive Center, n.d.). Therefore, MODIS-derived data are ill-suited in applications where real-time monitoring of atmospheric aerosols is required. These limitations ne-

cessitate better atmospheric aerosol measurement techniques that can provide readings with superior spatio-temporal resolutions compared to conventional AQM stations and satellite data. Hence, Vetres et al. (2010) concluded that more effective atmospheric aerosol monitoring can be achieved by using LIght Detection And Ranging (LIDAR).

LIDAR is an optical remote sensing technique that has high spatio-temporal resolution and is widely used in atmospheric research (Dong & Chen, 2017). Since LIDAR has its own light source, usually in the form of a pulsed laser transmitter, it can be deployed in almost any weather condition to conduct atmospheric scans. With the introduction of the single-pulse ruby laser by Maiman (1960) as a stable LIDAR light source and pioneering atmospheric studies conducted by Fiocco and Smullin (1963) using laser light sources, atmospheric LIDARs have been used extensively to conduct scans of the atmosphere and its constituent layers. Ground-based atmospheric LIDARs can be deployed to monitor atmospheric aerosols in mainly two orientations: vertical and horizontal directions. These two deployment methods are illustrated in Figure 1.2.

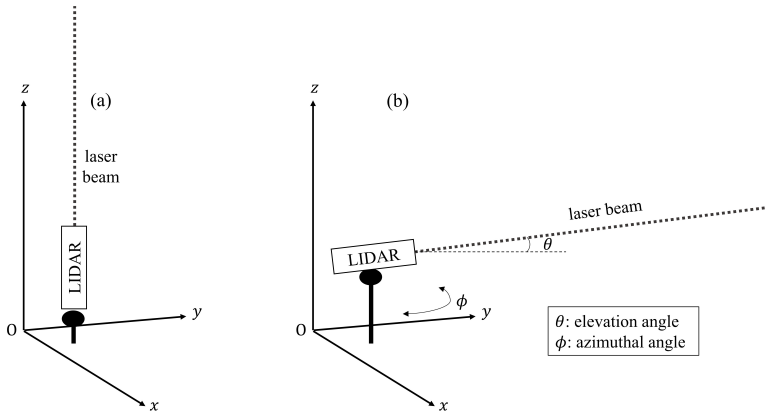

Figure 1.2: A comparison between (a) vertical and (b) horizontal scanning LIDAR. For horizontal scanning LIDAR, elevation angle is measured from the plane parallel to the surface to the LIDAR's scanning axis, while azimuthal angle refers to the rotation in the xy plane which is used in two-dimensional scans.

Vertical scanning LIDARs that point in the zenith direction are used to monitor aerosol layers that form within the troposphere during periods of poor air quality due to events like haze (refer Hee et al. (2014) and Jose et al. (2015)) and sand-

storms (refer Bedoya et al. (2016)). Jose et al. (2015) observed from vertical scanning LIDAR readings over Eastern India that during periods of heavier aerosol loading, the aerosol layers that have formed pushed the Planetary Boundary Layer (PBL) to a higher altitude. This observation was also confirmed by Hee et al. (2014) from vertical scanning LIDAR results obtained during the 2013 haze episode in Penang Island, Malaysia. Recognising the potential of using vertical scanning LIDARs to conduct large-scale aerosol studies, extensive LIDAR networks like European Aerosol Research LIDAR Network (EARLINET) (EARLINET, 2019), Latin American LIDAR Network (LALINET) (LALINET, 2019) and Micro-Pulse LIDAR Network (MPLNET) (Welton et al., 2001) have been established for coordinated, long-term atmospheric layer studies and monitoring. Although observing the evolution of aerosol layers and variations in PBL height during air pollution events seems like a possible method to use vertical scanning LIDARs in continuous atmospheric aerosol monitoring, this approach is poorly optimised because vertical scanning LIDARs are often immobile. The lack of acceptable horizontal spatial resolution as a result thereof means that vertical scanning LIDARs behave similarly to conventional AQM stations in terms of horizontal atmospheric aerosol monitoring. Thus, it is hoped that horizontal scanning LIDARs can compensate the limitations faced by their vertical counterparts.

Horizontal scanning LIDAR has been used in atmospheric aerosol detection only relatively recently compared to vertical scanning LIDAR. In this orientation, the LIDAR's scanning path is directed parallel or near-parallel to the ground in order to probe atmospheric aerosol concentrations in the horizontal plane. To avoid obstructions to the horizontal scanning LIDAR's scanning path, necessary precautions like installing the LIDAR unit on a tall building and introducing an elevation angle to the LIDAR's scanning direction are often required (Ma et al., 2019; Parracino et al., 2016; Xian et al., 2020). Since horizontal scanning LIDAR is capable of producing high quality range-resolved readings of extinction and/or backscattering coefficients which enables identification of regions with higher concentration of aerosols, this makes it a viable substitute to conventional AQM stations for monitoring atmospheric aerosol levels.

Horizontal scanning LIDARs can achieve cover large horizontal scanning regions of up to 10 km radially (Ma et al., 2019; Xian et al., 2020), hence horizontal scanning LIDARs can possibly provide wider coverage in real time compared to a similar number of AQM stations that are only able to provide localised point measurements. For example, He et al. (2012) used a horizontal scanning LIDAR to produce two-dimensional scans of the horizontal atmosphere over parts of Slovenia and Italy. Using the spatial maps of LIDAR readings, they were able to identify four individual aerosol sources which contributed to significantly higher LIDAR readings compared to the surrounding areas.

In recent years, the frequency of utilising horizontal scanning LIDARs to provide short-term atmospheric aerosol detection has increased in regions like China (refer Ma et al. (2019) and Xian et al. (2020)), Europe (refer He et al. (2012) and Parracino et al. (2016)) and the United States (refer Fortich et al. (2020)). This comes as no surprise since horizontal scanning LIDARs are expected to be more effective atmospheric aerosol monitoring probes compared to AQM stations, satellites, or even vertical scanning LIDARs. A summary of the different atmospheric aerosol monitoring methods mentioned in this section is shown in Figure 1.3.

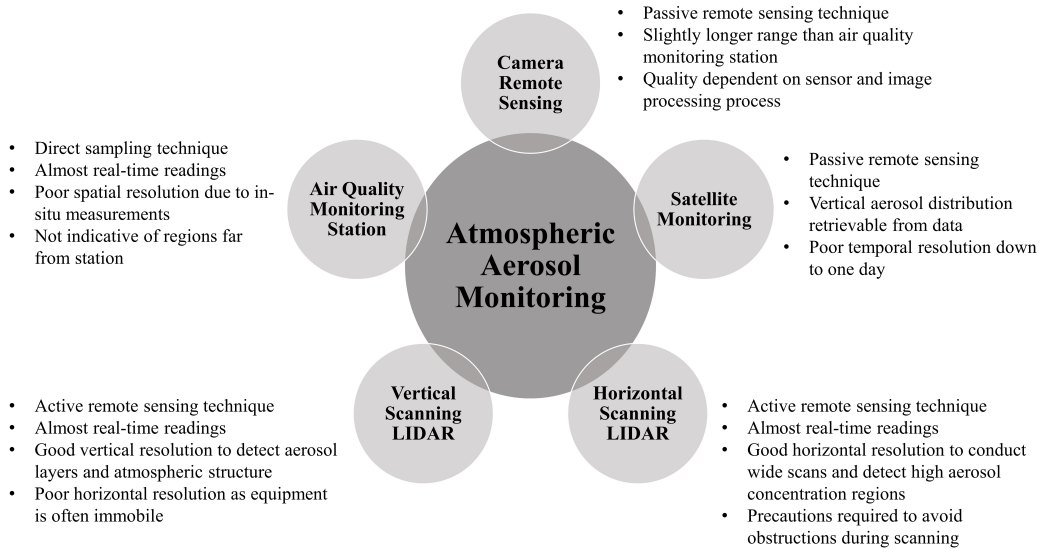

Figure 1.3: A comparison between AQM station, camera remote sensing, satellite monitoring, as well as vertical and horizontal scanning LIDAR in the context of atmospheric aerosol monitoring.

1.2 Problem Statement

Horizontal scanning LIDARs have exhibited greater potential in providing continuous atmospheric aerosol detection and monitoring than AQM stations due to their superior spatio-temporal resolution, larger effective detection range and faster detection times (Parracino et al., 2016). While horizontal scanning LIDARs have been adopted to carry out short-term detection of air pollution hotspots, their effectiveness in long-term, continuous atmospheric aerosol monitoring remains unknown since they are only relatively recently introduced. Consequently, there is a lack of numerical models available to establish empirical methods for using horizontal scanning LIDARs in long-term, continuous atmospheric aerosol detection and monitoring. Without appropriate numerical models, shortcomings due to poor design choices and possible limitations imposed by severe weather conditions on horizontal scanning LIDAR operation will be difficult to identify and address accordingly.

Since atmospheric LIDARs in general are complex and expensive to procure (Kovalev & Eichinger, 2004; Parracino et al., 2016; Spinhirne, 1993), it is impractical resource-wise to assess the feasibility of using horizontal scanning LIDAR for long-term, continuous atmospheric aerosol monitoring by purchasing physical equipment without establishing any appropriate theories or empirical methods. Furthermore, LIDAR as an active remote sensing technique will be susceptible to multiple scattering effects when the concentration of atmospheric aerosols increases, such as when haze worsens (Kovalev & Eichinger, 2004). This may affect the accuracy of LIDAR numerical models if multiple scattering processes and other possible factors like relative humidity (RH) are not taken into account.

1.3 Aim and Objectives

The aim of this study is to develop a numerical analysis of atmospheric aerosol monitoring using horizontal scanning LIDAR. This is achieved by evaluating LIDAR haze detection models that analyse the effects of PM present in haze on horizontal

scanning LIDAR readings. The objectives of this study are:

1. To develop an algorithm for horizontal scanning LIDAR design and simulation in any weather condition using real meteorological data.

2. To design a numerical assessment method used in performance evaluations of horizontal scanning LIDAR without physically assembling the unit, subject to case study requirements.

3. To formulate LIDAR haze detection models that incorporate multiple scattering LIDAR theory when analysing horizontal scanning LIDAR readings during non-hazy and hazy weather conditions.

4. To evaluate the stability of the LIDAR haze detection model against the influences of PM and factors like RH by using improved multiple scattering LIDAR theory.

1.4 Significance of the Study

This study uses numerical assessment methods to assess the feasibility of using horizontal scanning LIDARs as tools for long-term, continuous atmospheric aerosol monitoring via examination of LIDAR haze detection models. This powerful computational technique eliminates the need to assemble actual LIDARs for field tests and data acquisition. By constructing appropriate models and algorithms that accept real-life meteorological data as input parameters, expected horizontal scanning LIDAR readings can be simulated not just for the case study location of Universiti Sains Malaysia (USM), but also any regional setting, provided the necessary atmospheric parameters are available. Moreover, the novel numerical models used in assessing LIDAR designs and haze detection capabilities introduced in this study are generalised approaches that can be applied to any elastic backscatter LIDAR (EBL) to be used for atmospheric aerosol monitoring in the horizontal scanning direction. The versatility of the numerical models allows them to be used in other detailed numerical studies involving horizontal

scanning LIDARs as well as to form the basis of future empirical studies that concern long-term, continuous atmospheric aerosol monitoring.

This study considers a hypothetical dual-wavelength, multiple-receiver field-of-view (RFOV) horizontal scanning LIDAR as a case study example. Since the atmosphere is unique depending on the region and local climate, the conventional method used to evaluate LIDAR designs is by assembling LIDAR setups and comparing collected data to their expected results (Shiina, 2019; Tuan et al., 2017). However, this approach is resource-intensive and not feasible without significant amounts of funding. On the other hand, the hypothetical LIDAR that is designed and optimised using the numerical assessment methods presented in this study has been validated to have comparable performance to actual LIDAR setups that are used in the literature. These numerical assessment methods negate the requirement of a physical apparatus when developing and validating LIDAR designs or numerical models like LIDAR haze detection models, which can save a lot of time and resources during research.

Multiple scattering LIDAR theory is usually applied in cloud studies that employ the use of vertical scanning LIDARs (Pal & Carswell, 1976; Platt, 1973; Sassen & Petrilla, 1986). Contrastingly, this study incorporates multiple scattering LIDAR theory in a new setting: using horizontal scanning LIDAR to detect and characterise haze. The numerical assessment methods demonstrate that multiple scattering LIDAR theory can be used to describe the effects of PM on expected horizontal scanning LIDAR readings during haze. Furthermore, by making improvements to multiple scattering LIDAR theory, the versatility and applicability of the LIDAR haze detection model introduced in this study can be improved to accommodate the range of weather conditions that may take place in Malaysia.

1.5 Scope of the Study

In this study, the type of horizontal scanning LIDAR to be considered is limited to only ground-based EBLs, i.e. EBLs that are installed on the ground or on build-

ings, that are used for atmospheric aerosol detection and monitoring in the horizontal scanning direction. For this particular type of LIDAR, the wavelength of the received signal is unchanged due to elastic scattering processes that occur when the laser pulses transverse the atmosphere. While inelastic scattering processes like Raman scattering do occur (Gasmi, 2009; Weitkamp, 2006), EBLs are specially designed to perform spatial filtering on backscattered signals so that only signals which have wavelengths close to that of the laser transmitter used are recorded. This will be discussed in more detail in Chapter 2.

As mentioned in Section 1.4, this study will consider a dual-wavelength, multiple-RFOV horizontal scanning LIDAR as a case study example for haze detection and characterisation. This hypothetical LIDAR has both single scattering and multiple scattering EBL configurations, depending on the needs of the case study. Both daytime and nighttime operation will be simulated for the hypothetical LIDAR, but nighttime operation and its simulated results will be the main focus of the case study. Numerical analysis will be performed instead of using empirical data as the numerical assessment methods have been designed to negate the need for a physical LIDAR unit to conduct scans. To ensure that this hypothetical LIDAR has comparable performance to actual LIDARs used in atmospheric research, two examples from the literature will be used as reference performance indicators. More in-depth explanations and discussions will be covered in Chapter 3.

The case study location chosen for the numerical simulations and analysis is USM, Penang, Malaysia. This case study location is chosen as Penang is one of the states with the poorest air quality in Malaysia and is also where the author's institution is based at. Furthermore, there is previous research involving a vertical scanning LIDAR conducted in USM (refer Hee et al. (2014)), which can provide some reference information useful for the numerical analysis. Real-life meteorological data that can be obtained from government agency websites will be incorporated in the case studies. Specifically, data from the weather station in Bayan Lepas International Airport (BLIA) will be used in

the numerical analysis. Although BLIA is approximately 8 km away from USM, it is assumed that weather conditions do not differ greatly within a 10 km radius from the case study location. Therefore, the meteorological data that would have been collected in USM is assumed to be the same as that which is obtained from BLIA.

1.6 Thesis Structure and Overview

This thesis is organised as follows:

Chapter 1 is the introductory chapter that covers the background of the study and motivations behind the research. The reasons that lead to considering horizontal scanning LIDAR as a feasible tool and viable replacement to AQM stations in long-term, continuous atmospheric aerosol monitoring are presented. This chapter also outlines the problem statement, study aims and objectives, significance of the study as well as the scope of this research. An overview of the structure of the thesis is also presented in this chapter.

The next chapter, Chapter 2, comprises the literature review. This chapter covers single and multiple scattering LIDAR theory in the context of using EBL for atmospheric aerosol detection and monitoring. In particular, the theory behind the single and multiple scattering LIDAR equations for EBL is reviewed. This chapter also covers the considerations required when modelling horizontal scanning LIDAR. Input parameters and models that are essential to the numerical analysis such as the LIDAR ratio, multiple scattering correction factor, atmospheric model and LIDAR design specifications are examined. Lastly, this chapter is concluded with reviews of atmospheric aerosol detection and monitoring efforts using horizontal scanning LIDAR contained in the literature.

Next, Chapter 3 describes the first of a three-part methodology for the numerical analysis. In this chapter, the numerical assessment of horizontal scanning LIDAR performance via comparative study method is described. This numerical assessment method is used to design and evaluate the performance of the hypothetical horizontal

scanning LIDAR that is to be used as a case study example in this thesis. Evaluation criteria that will be used in the numerical assessment via comparative study as well as design specifications and considerations for the hypothetical LIDAR are detailed here. Then, two examples of atmospheric LIDARs are selected from the literature as part of the comparative study. Finally, this chapter ends with the generalised numerical assessment scheme and its simulation flowchart.

Chapter 4 is the second part of the methodology applied in the numerical analysis. The numerical model for haze detection using horizontal scanning LIDAR is detailed in this chapter. This model is used to assess the feasibility of using multiple scattering LIDAR theory when analysing horizontal scanning LIDAR readings to detect and characterise haze. This chapter describes how different concentrations of PM present during haze will affect expected horizontal scanning LIDAR readings via incorporation of multiple scattering LIDAR theory. Two suggested haze level indicators considered for constructing the LIDAR haze detection model are detailed. This LIDAR haze detection model can be generalised to any horizontal scanning LIDAR, hence Chapter 4 is concluded with its scheme and simulation flowchart.

The third and final part of the methodology for this numerical analysis is presented in Chapter 5. After establishing the LIDAR haze detection model in the previous chapter, multiple scattering LIDAR theory is improved to assess the effects of RH on horizontal scanning LIDAR readings during haze. This is because Malaysia is a humid country all year round, which may also be the case during haze episodes. This chapter outlines how hygroscopicity of aerosols, specifically PM, can be integrated into multiple scattering LIDAR theory when simulating expected LIDAR readings in different RH conditions. Improved multiple scattering LIDAR theory is used to design methods for identifying possible corrections to the LIDAR haze detection model when classifying dry and humid haze. This chapter is concluded with a general scheme of implementing the model corrections and the simulation flowchart.

Chapter 6 presents the results and discussion of the findings for this study. Here, simulation results from Chapter 3 are used to optimise and finalise the design of the hypothetical LIDAR. Then, this hypothetical LIDAR is used as a case study example to evaluate the numerical model for haze detection described in Chapter 4. The haze level indicators developed using multiple scattering LIDAR theory are inspected and assessed so that the LIDAR haze detection model can be established. The results are then interpreted using improved multiple scattering LIDAR theory described in Chapter 5 and the stability of the LIDAR haze detection model in the presence of variable RH is discussed.

Finally, this thesis is concluded in Chapter 7. This chapter summarises the key findings of the study and their implications towards using horizontal scanning LIDAR for long-term, continuous atmospheric aerosol monitoring. Some suggestions for future work are also provided in this chapter.

CHAPTER 2

REVIEW OF RELEVANT THEORIES AND STUDIES ON HORIZONTAL SCANNING LIDAR IN ATMOSPHERIC AEROSOL MONITORING

In this chapter, the relevant theories as well as research studies from the literature that are related to atmospheric aerosol monitoring using horizontal scanning LIDAR are reviewed. These theories form the basis of the numerical analysis in this study. The material in Sections 2.1 to 2.4 draws on the author's work (Ooi, Wong, & Edmund Loh, 2023a, 2023b; Ooi, Wong, Edmund Loh, & Teo, 2023; Ooi et al., 2025). In Section 2.1, single scattering LIDAR theory is explored to provide the background for deriving the single scattering LIDAR equation. This is followed by Section 2.2 that covers the theory of multiple scattering processes that are experienced by LIDAR in turbid media, which then leads to different proposed forms of the multiple scattering LIDAR equation. Next, theories and considerations needed when modelling input parameters for the numerical analysis are reviewed in Section 2.3. Lastly, this chapter is concluded with Section 2.4 which covers recent efforts to use horizontal scanning LIDAR in short-term atmospheric aerosol detection and monitoring.

2.1 Single Scattering LIDAR Theory

Interaction of light (photons) with matter (molecules and aerosols) in the atmosphere, primarily via elastic scattering processes, forms the operational basis of EBLs (Fujii & Fukuchi, 2005; Gasmi, 2009; Kovalev & Eichinger, 2004; Weitkamp, 2006). EBLs, and LIDARs in general, typically have a transmitter subsystem that produces laser pulses and a receiver-detector subsystem which detects pulses that are backscattered towards the LIDAR after interacting with matter in the atmosphere. Since light interacts differently with different types of molecules and atmospheric aerosols as it transverses the atmosphere, these varying degrees of scattering will be manifested in the signal recorded by the LIDAR. The LIDAR signal can then be inverted to obtain important optical parameters that reflect the constitution of the atmosphere. It is noted

that LIDAR, as a remote sensing technique, performs non-invasive, indirect sampling of atmospheric aerosols, hence the optical parameters obtained from LIDAR signals require certain calibrations to convert them into PM mass concentrations (Johnson, 1969; Richter, 1994; Rothe et al., 1974). Said calibrations will not be covered in this thesis as the numerical analysis described in this study will propose an alternative approach to using horizontal scanning LIDAR for atmospheric aerosol monitoring.

In the subsections that follow, insights into single scattering LIDAR theory that form the foundations of deriving the single scattering LIDAR equation will be presented. Subsection 2.1.1 will cover a review of the physical interactions that occur when LIDAR is used to conduct atmospheric aerosol detection and monitoring. Special emphasis will be put on elastic scattering processes. This is followed by Subsection 2.1.2 which contains an analysis of the assumptions and considerations made when developing the single scattering LIDAR equation. The terms in the single scattering LIDAR equation will also be described.

2.1.1 Physical Interactions in the Atmosphere

As previously mentioned, atmospheric LIDARs operate based on the interactions of transmitted light with matter present in the atmosphere along their scanning direction. These interactions often take place in the form of scattering processes, which depend on the relative length scales of the photon wavelength produced by the transmitter (oftentimes a laser), λ_{laser}, compared to the particle size, d, as well as the nature of scattering. Scattering of light has contributed to many phenomena that can be observed in everyday, for example the blueness of the daytime sky, its reddish hue in the evenings and the white glare observed around the Sun (Sirringhaus, 2020). For LIDARs, scattering processes both attenuate the laser beam that is directed into the atmosphere during LIDAR scans as well as backscatter the laser photons into the receiver to be collected for detection.

Scattering processes experienced by atmospheric LIDARs can primarily be divided into two types: elastic and inelastic scattering. As per its namesake, elastic scattering processes do not change the frequency of the incident radiation that has interacted with a particle at rest, which gives rise to the detection of signals using EBLs. Two types of elastic scattering processes dominate in the atmosphere, namely Rayleigh and Mie scattering. Rayleigh scattering takes place in the regime where the photon wavelength of radiation generated by the transmitter is significantly larger than the particle size ($\lambda_{\text{laser}} \gg d$). This is usually the case for atmospheric molecules like nitrogen and oxygen (Weitkamp, 2006). The Rayleigh scattering cross-section for small particles has a strong wavelength dependence which takes the form of $1/\lambda_{\text{laser}}^4$, hence radiation with shorter wavelengths will be scattered more strongly compared to those with longer wavelengths. When the laser wavelength is comparable to or smaller than the particle size ($\lambda_{\text{laser}} \lesssim d$), such as for atmospheric aerosols like PM, Mie scattering will occur. Unlike Rayleigh scattering, Mie scattering of radiation off of large particles has little to no dependence on its wavelength. According to Mie scattering theory, as the size of the scatterer increases with respect to (w.r.t.) to the wavelength of the incident radiation, the amount of scattering in the forward direction increases and becomes much greater than scattering in the backwards direction (Kovalev & Eichinger, 2004; Mie, 1908). This phenomenon is an essential component when discussing multiple scattering LIDAR theory. The scattering profiles for Rayleigh and Mie scattering are illustrated in Figure 2.1.

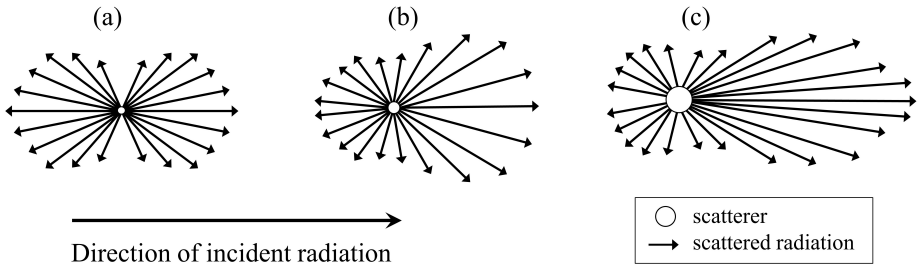

Figure 2.1: Differences between (a) Rayleigh and (b),(c) Mie scattering processes that occur in the atmosphere. The size of the scatterer increases from (a) to (c). The Mie scattering forward lobe is sharper and more intense for (c) than (b) due to the larger scatterer size.

For inelastic scattering processes like Raman scattering, part of the incident photon energy is absorbed by the vibrational-rotational modes of the interacting particles. This process can cause a large frequency shift in the detected backscattered photon (Gasmi, 2009; Weitkamp, 2006). Since the energy difference between initial and final states is specific to the interacting molecule, Raman scattering can be exploited to target certain molecules like methane and ozone (Houston et al., 1986; Philbrick & Mulik, 2000). However, Raman processes are very weak compared to Rayleigh scattering and can only be detected by specially designed Raman LIDARs. In addition to scattering processes, other physical processes such as Doppler shift, resonance fluorescence and differential-absorption can also take place, which lead to development of different types of LIDAR like Doppler LIDAR, high-spectral-resonance LIDAR and differential-absorption LIDAR (Fujii & Fukuchi, 2005; Gasmi, 2009; Kovalev & Eichinger, 2004; Weitkamp, 2006). These LIDARs are only mentioned for completeness and will not be discussed as they fall outside the scope of this thesis.

2.1.2 Derivation of the Single Scattering LIDAR Equation

There are several assumptions that need to be made in order to formulate the single scattering LIDAR equation (Fujii & Fukuchi, 2005; Gasmi, 2009; Kovalev & Eichinger, 2004; Weitkamp, 2006):

1. Assume that all scattering processes undergone by laser photons transmitted from the LIDAR are independent of each other due to random motion of the atmospheric scatterers.
2. Assume that only single scattering processes occur.
3. Assume that only elastic scattering processes occur.

From the first assumption, it follows that due to independent scattering processes, there are no phase correlations between the wavefunctions of the scattered photons. Therefore, one can simply add up the individual backscattered intensities of all the photons, which will then correspond to the total intensity of the detected laser beam.

The second assumption is only applicable in certain scenarios, as will be explained in Section 2.2. Here, multiple scattering processes are explicitly ignored because they are usually only prevalent when the atmosphere is turbid, such as in thick clouds, fogs and even haze. The third assumption is essential for EBLs which are the focus of this study. Under this assumption, there will be no frequency shift in the backscattered signal detected by EBLs, meaning the wavelength of the signal is the same as the transmitted laser wavelength.

It has been previously mentioned in Section 2.1 that a LIDAR consists of a transmitter and receiver-detector subsystem. Using the operational design of the LIDAR, the single scattering LIDAR equation can be derived by considering all possible physical processes and factors that will contribute to the intensity of the detected signal. This approach is more intuitive and easier to understand. Using this approach, one finds that power of a detected LIDAR signal can be expressed as the product of the following factors (Gasmi, 2009; Weitkamp, 2006):

1. The initial laser power, which is proportional to the number of photons produced by the laser.
2. The geometrical efficiency of the LIDAR due to its form factor.
3. The probability that any backscattered photons are successfully collected by the receiver optics.
4. The system efficiency of the LIDAR due to its optical and detector system.
5. The probability that the initial transmitted photons are backscattered towards the receiver optics.
6. The extinction of the laser beam from the LIDAR to the aerosol target.
7. The extinction of the laser beam from the aerosol target back to the LIDAR for detection.

Incorporating the factors mentioned above, the range-resolved single scattering LIDAR equation, $P_{\mathrm{SS}}(r)$, is therefore expressed according to Equation (2.1):

$$\begin{aligned} &P_{\mathrm{SS}}(r) \\ &= P_0\, q(r)\, \frac{A}{r^2}\, \eta\, \left[\beta_\pi(r)\, \Delta r\right]\, \exp\left[-\int_0^r \alpha\left(r', \lambda_{\mathrm{laser}}\right)\, \mathrm{d}r'\right]\, \exp\left[-\int_0^r \alpha\left(r', \lambda'\right)\, \mathrm{d}r'\right]. \end{aligned} \tag{2.1}$$

The terms are defined as follows:

$$\begin{aligned} P_0 &= \text{Initial laser power,} \\ r &= \text{LIDAR detection range,} \\ q(r) &= \text{LIDAR overlap function,} \\ A &= \text{Area of receiver,} \\ \eta &= \text{Total system efficiency,} \\ \beta_\pi(r) &= \text{Total backscattering coefficient,} \\ \Delta r &= \text{Thickness of sampled aerosol layer,} \\ \lambda_{\mathrm{laser}} &= \text{Initial laser wavelength,} \\ \alpha\left(r, \lambda_{\mathrm{laser}}\right) &= \text{Total extinction coefficient measured at } \lambda_{\mathrm{laser}}, \\ \lambda' &= \text{Backscattered laser wavelength,} \\ \alpha\left(r, \lambda'\right) &= \text{Total extinction coefficient measured at } \lambda'. \end{aligned}$$

There are several terms of interest in Equation (2.1). Firstly, $q(r)$, referring to the overlap function of the LIDAR setup, is used to describe how much of the transmitted laser beam is contained within the receiver field-of-view (RFOV) due to the LIDAR's geometrical constraints. This is because there will be a finite range within which the laser beam is not inside the scanning cone defined by the RFOV. Mathematically, the overlap function can be described using Equation (2.2):

$$q(r) = \begin{cases} 0 \le q(r) < 1 & \text{if } 0 \le r < r_0\,, \\ 1 & \text{if } r \ge r_0\,, \end{cases} \tag{2.2}$$

where r_0, commonly known as the full overlap distance, refers to the range at which full overlap between the laser beam and RFOV is achieved. Signals that are obtained within the region of incomplete overlap between laser beam and RFOV, $0 \leq r < r_0$, are often omitted from analyses as they may be corrupted because of near-field optical distortions (Kovalev & Eichinger, 2004).

The second term of interest, A/r^2, refers to the probability of a laser photon at distance r, after undergoing scattering processes, being collected by a receiver with aperture area A. This can also be interpreted as the solid angle subtended by the receiver from the laser photon. As r increases, the spatial probability of the receiver to be able to collect signals decreases as $1/r^2$. This inverse-square-range term, as well as $q(r)$, will determine the form of the LIDAR signal. At ranges close to the LIDAR, the signal power slowly increases from zero as the overlap becomes more complete, dictated by $q(r)$. At long ranges however, the signal strength decays rapidly due to the $1/r^2$ term.

Next, the total system efficiency, η, can be decomposed into two parts using the definition in Equation (2.3):

$$\eta = \eta_{\text{optical}} \times \eta_{\text{quantum}} \,. \tag{2.3}$$

Here, η_{optical} refers to the optical efficiency of the LIDAR system, while η_{quantum} refers to its quantum efficiency. The optical efficiency is affected by how well the receiver optics, for example the mirrors, lenses and filter that are used in the LIDAR, transmit the collected photons to the photosensor. Quantum efficiency, on the other hand, describes how well the photosensor reacts to the arrival of the individual photons. Quantum efficiency is defined as the average number of photoelectrons generated per incident photon (Kovalev & Eichinger, 2004). Both η_{optical} and η_{quantum} can be expressed in decimals or percentages and by definition cannot exceed efficiencies of 100%. This means that careful choice of optical components and photosensors is key to optimising the signal strength that can be detected and output by the LIDAR.

$\beta_\pi(r)\,\Delta r$ defines the probability that the initial laser photons are backscattered towards the receiver. The total backscattering coefficient, $\beta_\pi(r)$, has a subscript π which indicates that only photons that are scattered through an angle of π radians from their original flight path are of interest as these photons have the highest probability of returning to the LIDAR. The thickness of the aerosol layer sampled by the LIDAR, denoted as Δr, is equal to $c\,\tau/2$, where c is the speed of light and τ is the duration of the laser pulse. This can be understood by considering the relationship between the time measured by LIDAR and position of the aerosol target: Suppose that the aerosol target is located between positions r_1 and r_2. The thickness of the aerosol layer, $\Delta r = r_2 - r_1$ must be related to τ. Since the photons produced by the LIDAR must travel to and from the aerosol target in order to be detected, Equation (2.4) holds:

$$2r = c\,t\,, \tag{2.4}$$

such that r is some position away from the LIDAR and t is the time of detection. Suppose then t_1 is the time when a signal from r_1 is detected and t_2 corresponds in the same way to r_2, one then obtains Equations (2.5) and (2.6):

$$2r_1 = c\,t_1\,, \tag{2.5}$$

$$2r_2 = c\,t_2\,. \tag{2.6}$$

Assuming that the detection of laser pulses is instantaneous, then the minimum temporal separation must be equal to the duration of the laser pulse. As a result, $t_2 - t_1 = \tau$. Using this relation together with Equations (2.5) and (2.6), one obtains Equation (2.7):

$$\begin{aligned} \Delta r &= r_2 - r_1 \\ &= \frac{c}{2}\,(t_2 - t_1)\,, \\ \therefore\ \Delta r &= \frac{c\,\tau}{2}\,. \end{aligned} \tag{2.7}$$

Therefore, an additional factor of $1/2$ in the result for Δr arises due to the apparent backfolding the pulse as it travels to and from the aerosol target (Fujii & Fukuchi, 2005; Gasmi, 2009; Kovalev & Eichinger, 2004; Weitkamp, 2006).

The last two terms in Equation (2.1) describe the attenuation of the laser beam as it propagates through the atmosphere. The exponential form is the result of the Beer-Lambert extinction for LIDARs (Weitkamp, 2006). $\exp\left[-\int_0^r \alpha\,(r', \lambda_{\text{laser}})\ \mathrm{d}r'\right]$ describes the extinction of the laser beam travelling towards the aerosol target. Since there is yet to be any interaction between the laser photons and the aerosol, the initial wavelength, λ_{laser}, is unchanged. After the laser pulses have interacted with the aerosol, there may be changes in wavelength due to the processes described in Subsection 2.1.1. For completeness, the laser beam is assumed to have a new wavelength, λ', which gives rise to the return extinction, $\exp\left[-\int_0^r \alpha\,(r', \lambda')\ \mathrm{d}r'\right]$.

Using the third assumption mentioned at the beginning of Subsection 2.1.2, since only elastic scattering processes are considered, there will be no difference between the initial and backscattered laser wavelengths. Under this assumption, $\lambda_{\text{laser}} = \lambda'$. Hence, one can remove the wavelength dependency from the total extinction coefficients. The total extinction coefficient, $\alpha(r)$, is then redefined according to Equation (2.8):

$$\alpha(r) = \alpha\,(r, \lambda_{\text{laser}}) = \alpha\,(r, \lambda') \quad \text{if } \lambda_{\text{laser}} = \lambda'\,. \tag{2.8}$$

As a result, one can combine the two exponential terms to form a single two-way transmittance term (Fujii & Fukuchi, 2005; Gasmi, 2009; Kovalev & Eichinger, 2004). This is given by Equation (2.9):

$$\exp\left[-2\int_0^r \alpha(r')\,\mathrm{d}r'\right] = \exp\left[-\int_0^r \alpha\,(r', \lambda_{\text{laser}})\ \mathrm{d}r'\right]\exp\left[-\int_0^r \alpha\,(r', \lambda')\ \mathrm{d}r'\right] \quad \text{if } \lambda_{\text{laser}} = \lambda'\,. \tag{2.9}$$

Oftentimes, a term called the LIDAR constant, C_0, is used to summarise the overall system performance for a LIDAR. This term is related to the laser pulse energy, E_0, via Equation (2.10):

$$C_0 \equiv P_0\,\frac{c\,\tau}{2}\,A\,\eta = E_0\,\frac{c}{2}\,A\,\eta\,. \tag{2.10}$$

Now, combining the results from Equations (2.1), (2.7), (2.9) and (2.10), one will obtain the more recognisable form of the single scattering LIDAR equation. This is shown in Equation (2.11):

$$P_{\mathrm{SS}}(r) = C_0 \frac{q(r)}{r^2} \beta_\pi(r) \exp\left[-2 \int_0^r \alpha\,(r')\ \mathrm{d}r'\right]. \tag{2.11}$$

For completeness, additional contributions to the detected LIDAR signal need to be considered. These contributions usually take the form of background noise, P_B, as well as detector noise, P_D. Therefore, the total expected signal strength for a single scattering EBL, $P_{\mathrm{SS,total}}(r)$, is given as Equation (2.12):

$$\begin{aligned} P_{\mathrm{SS,total}}(r) &\equiv P_{\mathrm{SS}}(r) + P_B + P_D \\ &= C_0 \frac{q(r)}{r^2} \beta_\pi(r) \exp\left[-2 \int_0^r \alpha\,(r')\ \mathrm{d}r'\right] + P_B + P_D\,. \end{aligned} \tag{2.12}$$

Equation (2.12), represented by Figure 2.2, will form an integral part of the numerical analysis described in this thesis.

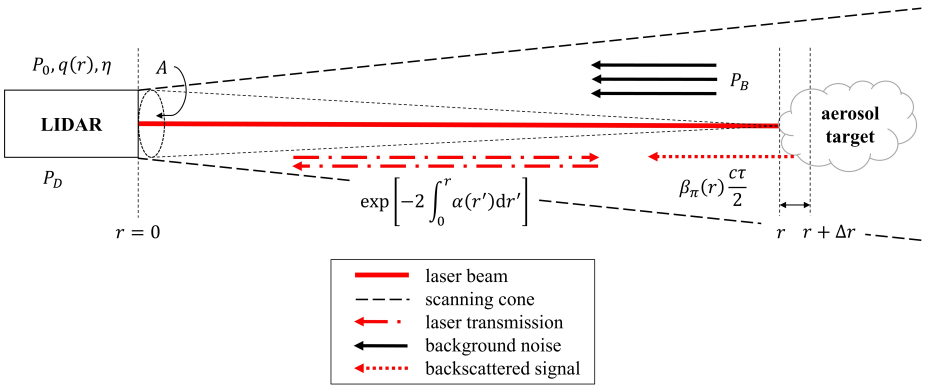

Figure 2.2: A diagrammatic representation of the various terms that contribute to the expression of the single scattering LIDAR equation.

2.2 Multiple Scattering LIDAR Theory

In Section 2.1, the derivation of the single scattering LIDAR equation has been presented. From the literature, it can be observed that this equation suffices for most practical and simulation applications (Parracino et al., 2016; Shiina, 2019; Tuan et al.,